

Supporting Information (SI)

Experimental section

1. Materials preparation

We prepared the HEO-supported HEA clusters by an alloying-dealloying method. The multicomponent precursor alloys such as $\text{Al}_{94}\text{Ni}_1\text{Co}_1\text{Fe}_1\text{Cr}_1\text{Mo}_1\text{Ti}_1$, $\text{Al}_{93.8}\text{Ni}_1\text{Co}_1\text{Fe}_1\text{Cr}_1\text{Mo}_1\text{Ti}_1\text{Pt}_{0.2}$, $\text{Al}_{93.79}\text{Ni}_1\text{Co}_1\text{Fe}_1\text{Cr}_1\text{Mo}_1\text{Ti}_1\text{Pt}_{0.03}\text{Pd}_{0.03}\text{Au}_{0.03}\text{Ag}_{0.03}\text{Cu}_{0.03}\text{Ir}_{0.03}\text{Ru}_{0.03}$, etc., were prepared firstly by a melt-spinning method. Specifically, noble metals (if contains) were firstly fused together, and then alloyed with non-noble metals. All these precursor alloys were prepared by melting pure metals (> 99.9 wt%) in an induction-melting furnace under the protection of Ar. The prepared alloys were then melted again in the quartz tube and injected into the air to contact the high-speed rotating copper roller to produce the alloy strips with a thickness of about 25 μm and a width of about 2 mm. The tangential velocity of the drum was about 30 m s^{-1} , and the injection gas pressure was 300-400 Pa to obtain alloy strips. Then, the precursor alloy strips were etched in 0.5 M NaOH solution for about 12 hours to obtain the nanostructured high entropy alloy@oxides, or pure high-entropy oxides. The dealloyed samples were washed with water and ethanol for several times and stored in a dry N_2 -protected environment.

To prepare uniform catalyst ink, 4 mg of catalyst (the dealloyed samples), 3 mg of carbon nanotubes, 300 μL isopropanol and 100 μL Nafion (0.5 wt%) were ultrasonically mixed together for 15 minutes. Before the electrochemical test, the catalyst ink (about 5 μL) was evenly coated on glassy carbon electrodes (diameter: 4 mm) and dried under an infrared lamp for more than 5 minutes until the catalyst was firmly attached to the electrode. Reference materials used (Pt/C, IrO_2 , etc.) and all the chemicals were purchased from Aladdin Industrial Corporation. The use of carbon materials such as carbon nanotube was mainly to further enhance the conductivity of the catalyst ink. The added carbon nanotube also helps the catalyst ink to form a uniform film coated on current collectors such as glassy carbon or carbon cloth.

2. Materials characterization

Characterization of these samples were performed by an XRD diffractometer using Cu K α radiation (Rigaku D/Max 2500), an X-ray photoelectron spectroscopy (XPS) recorded with an Al K α X-ray source (ESCALAB 250), a scanning electron microscopy (SEM, HITACHI S-4700) and a transmission electron microscopy (JEM-2100F) equipped with energy dispersive X-ray spectrometer (EDS). The atomic details of the nanoclusters were explored by aberration-corrected high-angle annular dark field scanning transmission electron microscopy (HAADF-STEM). The Brunauer-Emmett-Teller (BET) surface area was evaluated by N₂ adsorption/desorption isotherms conducted on a Quantach-rome Autosorb-3B surface analyzer.

3. Electrochemical measurements

Electrochemical measurements were carried out on an electrochemical workstation (CH Instruments 760E) at room temperature with a three-electrode system including a modified glassy carbon electrode as working electrode, a carbon rod as the counter electrode and an Ag/AgCl (filled with saturated KCl solution) as the reference electrode. 1 M KOH saturated with O₂ was used as electrolyte solution for oxygen evolution reaction (OER) and 0.1 M KOH solution saturated with O₂ was used for oxygen reduction reaction (ORR). Linear scan voltammograms were conducted with a scan rate of 5 mV s⁻¹. Electrical impedance spectroscopy was carried out under the following conditions: ac voltage amplitude: 5 mV, frequency ranges: 100 KHz to 0.01 Hz, and open circuit. The current density was normalized according to the geometrical area, and the measured potentials were converted to a reversible hydrogen electrode (RHE) scale according to the Nernst equation ($E_{\text{RHE}} = E_{\text{Ag/AgCl}} + 0.059 \cdot \text{pH} + 0.1976$); the overpotential (η) for OER was calculated according to the following formula: η (V) = $E_{\text{RHE}} - 1.23$ V.

4. Assembling and testing of Zn-air batteries

The liquid Zn-air battery was assembled using the catalyst modified breathable carbon cloth (total catalyst mass loading of ~ 0.5 mg cm⁻²) as the air cathode, a polished

zinc plate (thickness of 0.1 mm) as the anode, and 6.0 M KOH containing 0.2 M Zn(OAc)₂ applied as the electrolyte. The effective exposed area of the cathode to the air is ~1 cm². The Pt/C-IrO₂-based battery was assembled using the same method for reference.

5. Density functional theory calculation

The spin-polarized density functional theory (DFT) computations were performed using the Vienna ab initio Simulation Package (VASP).^{1,2} We used the Perdew-Burke-Ernzerhof (PBE) functional and the projector augmented wave (PAW) pseudopotentials.^{3,4} The energy cutoff was 450 eV. The simulated models contained 4 layers for all simulations. The thickness of vacuum was 15 Å to minimize the artificial interactions among the supercell images. All the atomic structures were fully relaxed until the forces on each atom being less than 0.02 eV/Å and the energy variation between two iterations being less than 1×10⁻⁵ eV. During the structural relaxation, only the atoms in the top two surface layers were relaxed to mimic the structure of a semi-infinite solid. The Brillouin zone of each slab was sampled by a Monkhorst-Pack k-point mesh of 4 × 4 × 1 for geometry optimization and an 8 × 8 × 1 k-mesh for density of states (DOS) calculations.

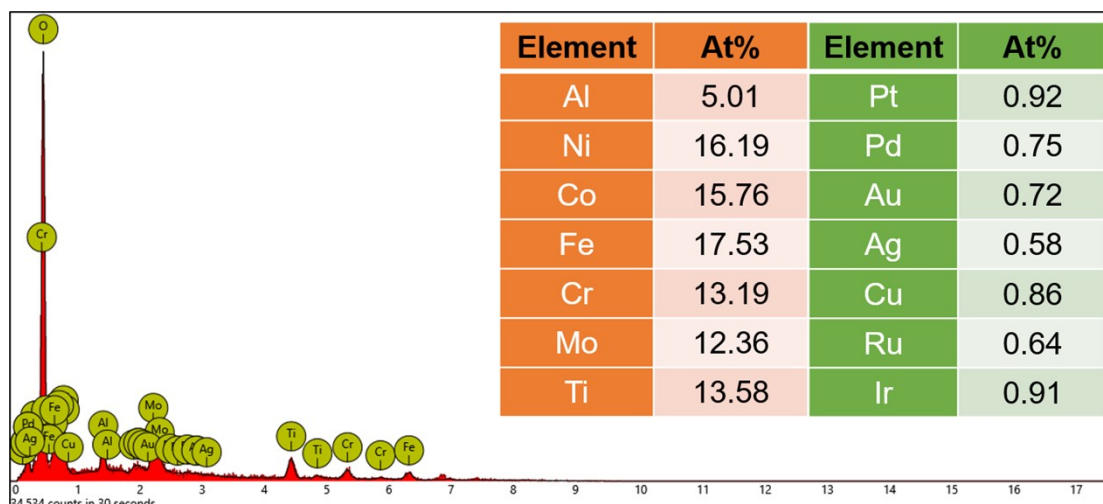


Fig. S1. EDS analysis result of the dealloyed HEA Cluster@HEO sample.

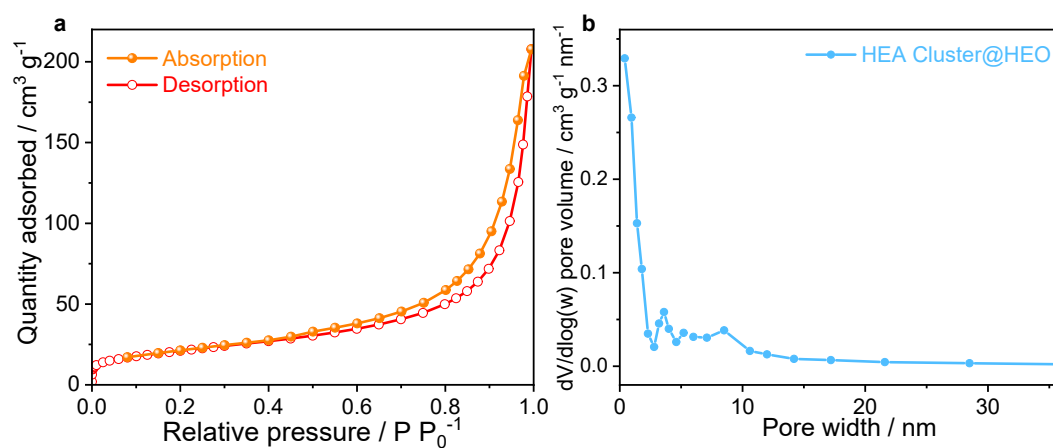


Fig. S2. (a) N_2 adsorption–desorption isotherms and (b) pore size distribution of the dealloyed HEA Cluster@HEO sample.

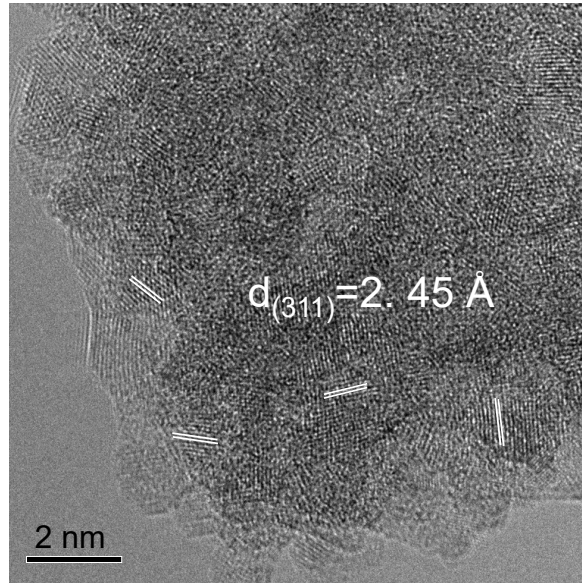


Fig. S3. HRTEM image of the HEA Cluster@HEO. Spinel nanocrystals are identified.

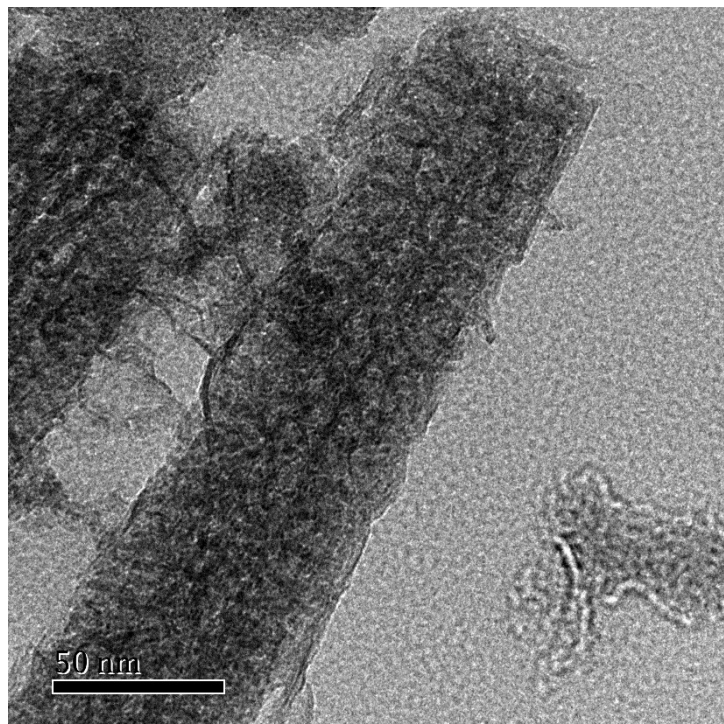


Fig. S4. TEM image of the HEA Cluster@HEO nanowires. The clear contrast indicates the nanoporous structure of the etched Al_3X nanowire-like structure.

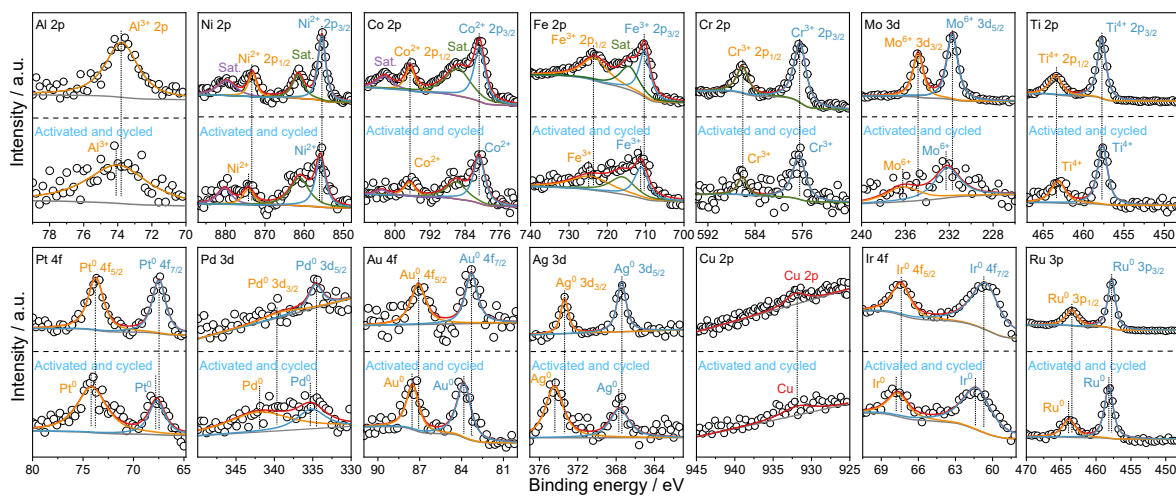


Fig. S5. XPS spectrum of each element in the HEA Cluster@HEO sample before and after battery cycling.

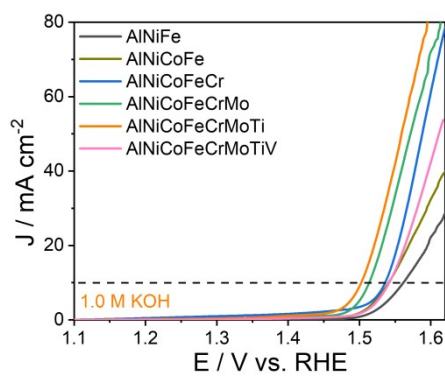


Fig. S6. OER polarization curves of the prepared multicomponent HEOs.

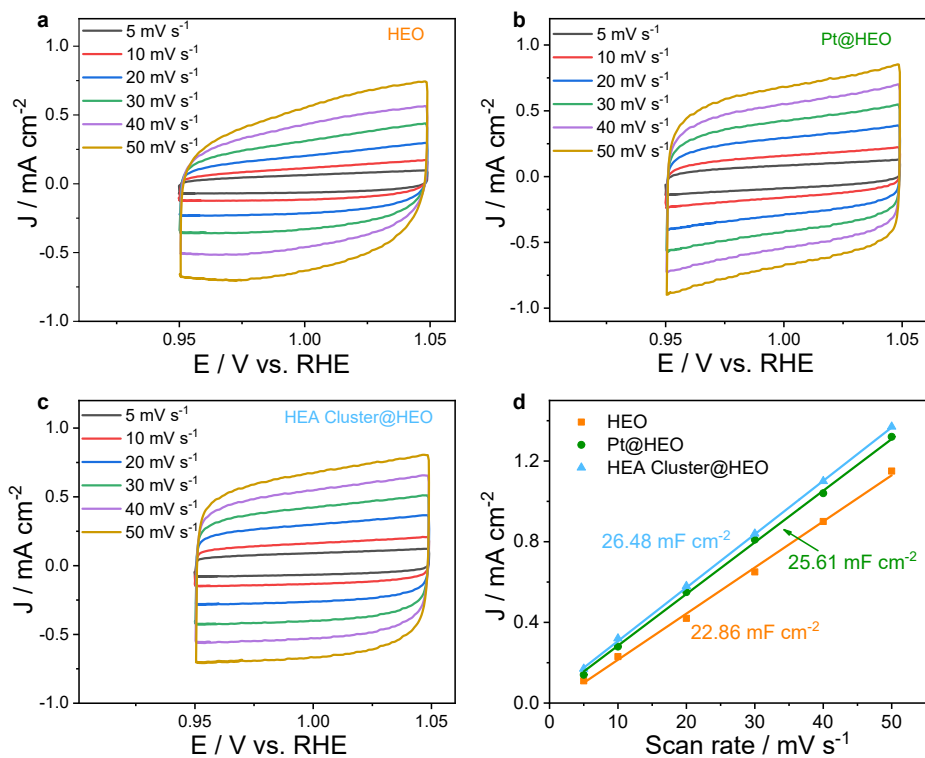


Fig. S7. (a) CV curves of HEO, (b) Pt@HEO, (c) HEA Cluster@HEO in 1.0 M KOH in the potential of 0.95-1.05 V vs. RHE at various scan rates (5, 10, 20, 30, 40 and 50 mV s^{-1}). (d) Corresponding plots of current density differences ($\Delta J/2$) vs. scan rate at 1.0 V. The slope is equivalent to the double-layer capacitance C_{dl} .

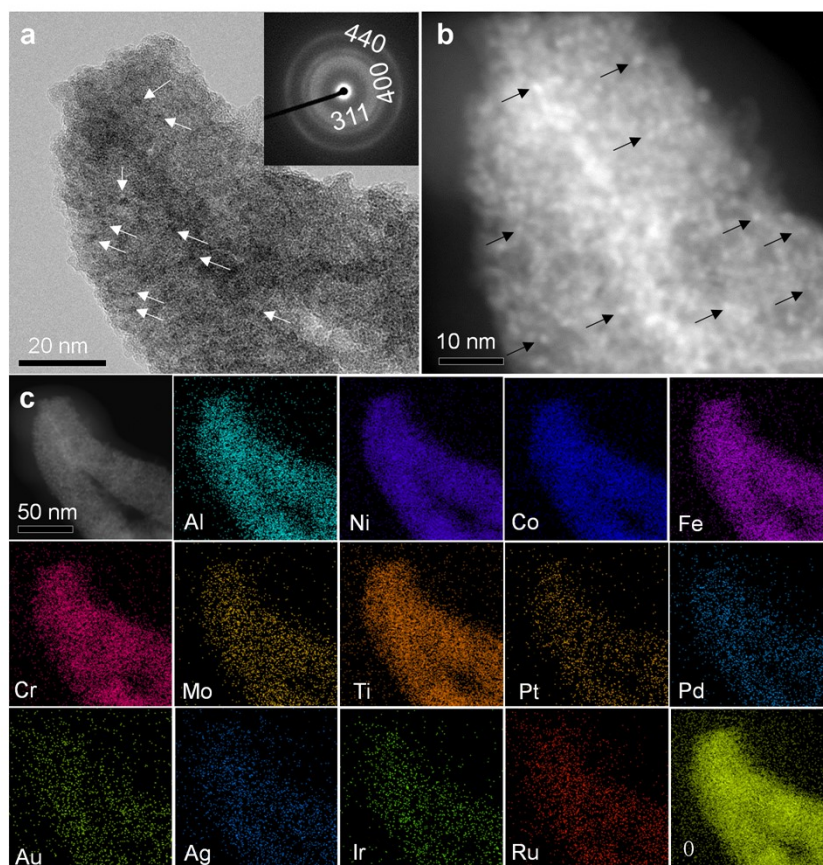


Fig. S8. (a) TEM, (b) HAADF-STEM images and (c) STEM-EDS mapping of the HEA Cluster@HEO after battery tests. Some HEA clusters are indicated by arrows.



Fig. S9. The open circuit voltage of the Pt/C-IrO₂-catalyzed battery.

Table S1. Comparison of OER activities with recent reported electrocatalysts in alkaline electrolytes.

Catalysts	Mass Loading ($\mu\text{g cm}^{-2}$)	Overpotential @10 mA/cm ² (mV)	Tafel slope (mV dec ⁻¹)	Refs.
HEA Cluster@HEO	39.5 (noble metal)	240	49.3	This work
	8.3 (Pt)			
Pt@HEO	42.8 (Pt)	265	52.8	This work
IrO₂	145.7 (Ir)	295	66.4	This work
Ru-CoV-LDH/NF	51.6 (Ru)	240	81.2	<i>ChemSusChem</i> 2021, 14, 730 – 737
Co-RuIr	135.5 (Ru/Ir)	250	66.9	<i>Adv. Mater.</i> 2019, 31, 1900510
1D-RuO ₂ -CNx	2500 (RuO ₂)	260	56	<i>ACS Appl. Mater. Interfaces</i> 2016, 8, 28678–28688
RuO ₂ /N-C	240(Ru)	280	56	<i>ACS Sustainable Chem. Eng.</i> 2018, 6, 11529– 11535
PdIr UNWs/WFG	~200 (Pd/Ir)	280	57.5	<i>Nanoscale</i> 2019, 11, 14561–14568
Mn/Fe-HIB-MOF	150	280	45	<i>Energy Environ. Sci.</i> 2019, 12, 727–738
Ni _{0.93} Ir _{0.07} /rGO	19.64 (Ir)	290	55.9	<i>J. Energy Chem.</i> 2020, 49, 166–173
Co@Ir/NC-10%	202 (Ir)	292	73.8	<i>ACS Sustainable Chem. Eng.</i> 2018, 6, 5105–5114
Ir1@Co/NC	4.4 (Ir)	373	163	<i>Angew. Chem., Int. Ed.</i> 2019, 58,

PtLaNiCoFe HEMG-
NP

303 (Pt)

377

150

Table S2. Comparison of the ORR activities with recent reported materials in 0.1 M KOH.

Catalysts	E_{onset} (V vs. RHE)	E_{1/2} (V vs. RHE)	Refs.
HEA Cluster@HEO	1.01	0.89	This work
Pt@HEO	0.99	0.855	This work
20% Pt/C	0.98	0.86	This work
PtCo@NC-10	1.02	0.92	<i>Nano Res.</i> 2017, 10, 3228-3237
ZIF-L-D-Co ₃ O ₄ /CC	1.01	0.90	<i>Adv. Sci.</i> 2019, 6, 1802243
R-PtN Ws	1.00	0.87	<i>Science</i> 2016, 354, 6318
FeNi/N-CPCF-950	0.99	0.867	<i>Appl. Catal. B</i> 2020, 263, 118344
Mn/Fe-HIB-MOF	0.99	0.883	<i>Energy Environ.</i> <i>Sci.</i> 2019, 12, 727– 738
Pt-Co/NC	0.98	0.87	<i>ACS Appl. Nano</i> <i>Mater.</i> 2018, 1, 3331-3338
Ru@NGT	0.97	0.83	<i>ACS Appl. Energy</i> <i>Mater.</i> 2019, 2, 10, 7330–7339
Pt/Fe-NC-900	0.96	0.864	<i>Energy Fuels</i> 2020, 34, 11527–11535
Ru-N/G-750	0.94	0.82	<i>ACS Nano</i> 2017, 11, 7, 6930–6941

Pd-Ru@NG	0.92	0.81	<i>Chem. Commun.</i> 2019,55, 13928- 13931
----------	------	------	--

Table S3. Comparison of activities with recent reported bifunctional electrocatalysts in alkaline electrolytes.

Catalysts	Overpotential @10 mA cm ⁻² (mV)	E _{1/2} (V vs. RHE)	Refs.
HEA Cluster@HEO	240	0.89	This work
Pt@HEO	265	0.85	This work
S, N-Fe/N/C-CNT	370	0.85	<i>Angew. Chem. Int.</i> <i>Ed.</i> 2017, 56, 610–614
FeCo@MNC	245	0.86	<i>Appl. Catal. B</i> 2019, 244, 150–158
CoNi@NCNT/NF	310	0.87	<i>Adv. Energy Mater.</i> , 2018, 8, 1800480
Co-Co ₃ O ₄ /C	330	0.88	<i>Chem. Commun.</i> 2019, 55, 2924–2927
CuS/NiS ₂	300	0.89	<i>Adv. Funct.</i> <i>Mater.</i> 2017, 27, 1703779
Co@NHCC-800	280	0.837	<i>Appl. Catal. B</i> 2019, 254, 55–65
Co@N-CNTF	350	0.81	<i>J. Mater. Chem. A</i> 2019, 7, 3664–3672
ZIF-L-D-Co ₃ O ₄ /CC	310	0.9	<i>Adv. Sci.</i> 2019, 6, 1802243
Co _{0.85} Se@NC	230	0.817	<i>J. Mater. Chem. A</i> 2017, 5, 7001–7014

Table S4. Comparison of the liquid Zn-air battery performance of this work with recent reported literature data.

Catalysts	Open circuit potential (V)	Peak power density (mW cm ⁻²)	Ref.
HEA Cluster@HEO	1.528	146.4	This work
Pt/C-IrO₂	1.462	103.8	This work
ZIF-L-D-Co ₃ O ₄ /CC	1.66	75	<i>Adv. Sci.</i> 2019, 6, 1802243
Fe ₂₀ @N/HCSs	1.57	140.8	<i>Adv. Funct. Mater.</i> 2020, 30, 2005834
mPtPd-NF	1.52	111	<i>ACS Sustainable Chem. Eng.</i> 2018, 6, 12367–12374
P, S-carbon nitride sponges (CNS)	1.51	198	<i>ACS Nano</i> 2017, 11, 347
(Zn,Co)/NSC	1.5	150	<i>Nano Energy</i> 2019, 58, 277-283
NiCo ₂ S ₄ /N-CNT	1.49	147	<i>Nano Energy</i> 2017, 31, 541–550
Co/N-PCC	1.48	127.8	<i>J. Catal.</i> 2019, 369, 143–156
N-GCNT/FeCo	1.48	89	<i>Adv. Energy Mater.</i> 2017, 7, 1602420
FeNi/N-CPCF-950	1.478	160.6	<i>Appl. Catal. B</i> 2020, 263, 118344
C-MOF-C2-900	1.46	105	<i>Adv. Mater.</i> 2018, 30, 1705431
CoSAs@NC	1.46	105.3	<i>Angew. Chem. Int. Ed.</i> 2019, 58, 1-7
Co/Co ₃ O ₄ @PGS	1.45	118.27	<i>Adv. Energy Mater.</i> 2018, 8, 1702900

Mn/Fe-HIB-MOF	1.442	194	<i>Energy Environ. Sci.</i> 2019, 12, 727–738
CuS/NiS ₂ INs	1.44	172.4	<i>Adv. Funct. Mater.</i> 27, 2017, 1703779
Fe _{0.5} Co _{0.5} O _x / N- doped reduced graphene oxide (NrGO)	1.44	86	<i>Adv. Mater.</i> 2017, 29, 1701410
Co-N ₃ B-CSs	1.43	100.4	<i>ACS Nano</i> 2018, 12, 1894-1901.
Ni ₃ FeN/Co ₃ N-CNF	1.43	200	<i>Nano Energy</i> 2017, 40, 382–389
CoPx@CNS	1.40	110	<i>Angew. Chem. Int. Ed.</i> 2020, 59, 21360-21366
Co ₄ N/CNW/CC	1.35	174	<i>J. Am. Chem. Soc.</i> 2016, 138, 10226

Table S5. Loading amounts of different noble metals in HEA Cluster@HEO andPt@HEO sample. ($\mu\text{g cm}^{-2}$)

Sample \ Elements	Pt	Pd	Au	Ag	Ir	Ru	Total
HEA Cluster@HEO	8.3	5.4	7.1	6.3	7.6	4.8	39.5
Pt@HEO	42.8						42.8

6. Reference

1. G. Kresse and J. Furthmuller, *Comp. Mater. Sci.*, 1996, **6**, 15-50.
2. G. Kresse and J. Furthmuller, *Phys. Rev. B*, 1996, **54**, 11169-11186.
3. J. P. Perdew, K. Burke and M. Ernzerhof, *Phys. Rev. Lett.*, 1996, **77**, 3865-3868.
4. G. Kresse and D. Joubert, *Phys. Rev. B*, 1999, **59**, 1758-1775.